BIOCHEMISTRY
including biophysical chemistry & molecular biology

Rapid Report

pubs.acs.org/biochemistry

Analysis of the Radiation-Damage-Free X-ray Structure of Photosystem II in Light of EXAFS and QM/MM Data

Mikhail Askerka,[†] David J. Vinyard,[†] Jimin Wang,[‡] Gary W. Brudvig,*[,†] and Victor S. Batista*[,†]

[†]Department of Chemistry, Yale University, New Haven, Connecticut 06520-8107, United States,

[‡]Department of Molecular Biophysics and Biochemistry, Yale University, New Haven, Connecticut 06520-8114, United States

Supporting Information

ABSTRACT: A recent femtosecond X-ray diffraction study produced the first high-resolution structural model of the oxygen-evolving complex of photosystem II that is free of radiation-induced manganese reduction (Protein Data Bank entries 4UB6 and 4UB8). We find, however, that the model does not match extended X-ray absorption fine structure and QM/MM data for the S_1 state. This is attributed to uncertainty about the positions of oxygen atoms that remain partially unresolved, even at 1.95 Å resolution, next to the heavy manganese centers. In addition, the photosystem II crystals may contain significant amounts of the S_0 state, because of extensive dark adaptation prior to data collection.

Photosystem II (PSII) is a protein-pigment complex responsible for the production of oxygen in higher plants, algae, and cyanobacteria during the light reactions of photosynthesis.[1,2] In PSII, the evolution of oxygen proceeds through the catalytic reaction of water oxidation.[3,4] This process is initiated by absorption of a photon by the chlorophylls called P_{680}, leading to charge separation across the thylakoid membrane. The charge-separated state containing $P_{680}^{+\bullet}$ oxidizes a nearby tyrosine species (Y_Z) to form $Y_Z^{\bullet}$, which in turn oxidizes the oxygen-evolving complex (OEC). The OEC is a $CaMn_4O_5$ cluster in which the metal atoms are connected through μ-oxo bridges, forming a cuboidal $CaMn_3O_4$ core with a dangling Mn.[5,6] As the catalytic cycle proceeds, the OEC accumulates oxidizing equivalents, thus evolving through the storage states S_n (n = 0−4).[4,7] During each turn of the cycle, two water molecules are transformed into O_2, while four protons are released to the thylakoid lumen, and plastoquinone is reduced to plastoquinol on the acceptor side. The OEC oxidizes water efficiently at low overpotentials,[8] which makes it a prototype for artificial homogeneous and heterogeneous water oxidation catalysts.

X-ray diffraction (XRD) has been an important method for gaining structural information about the OEC and its surroundings.[5,9−13] Over the past decade, the resolution of XRD experiments has improved from 3.8 to 1.9 Å, revealing the atomic coordinates of the OEC atoms as well as the ligation scheme of coordinated residues and water molecules.[5] To date, however, all XRD structures that utilized synchrotron radiation have suffered from radiation damage from the X-ray source, leading to Mn reduction.[14] These structures of the OEC, including the 1.9 Å resolution structure by Shen and co-workers,[5] have Mn−Mn distances that are longer than those predicted by extended X-ray absorption fine structure (EXAFS) spectroscopy,[15−18] and computational methods, including density functional theory and quantum mechanics/molecular dynamics (QM/MM).[16,19]

Radiation damage has been recently avoided by using femtosecond X-ray free electron laser crystallography, a process in which a single diffraction pattern is collected from either a single small crystal (or a section of a larger crystal), using very short and very high-energy X-ray pulses.[20,21] Yano, Yachandra, and co-workers as well as Fromme and co-workers have used this method to study small (≤10 μm) dark-adapted PSII crystals (presumably prepared in the S_1 state) and have reported structural models at 6.5 Å,[22] 5.7 Å,[23] 5.0 Å,[24] and 4.9 Å resolution.[25] By flashing these small crystals with visible light before collecting diffraction patterns, they have reported putative S_2,[23,25] S_3,[24,25] and S_0[25] models. However, the intrinsic low resolution of the diffraction pattern has thus far prevented conclusions about changes in the OEC structure. Calculations of electron density difference Fourier maps,[23] based on S_1 and S_2 QM/MM models, however, have shown that the $S_1 \rightarrow S_2$ transition primarily involves changes in the environment of the dangling Mn (Mn4).[26]

Recently, Shen and co-workers used large dark-adapted PSII crystals (1.2 mm × 0.5 mm × 0.2 mm) to generate a "radiation-damage-free" PSII model at 1.95 Å resolution.[6] While X-ray-induced Mn reduction is not an issue for this improved OEC structure, in the work presented here, we show that the simulated EXAFS spectrum of this OEC structure does not match experimental measurements of the S_1 state.[18] We attribute these differences to uncertainty in the positions of the light oxygen atoms, which are not sufficiently resolved even at 1.95 Å resolution, next to the heavy manganese centers (Figure 1A, B). In addition, contributions from the S_0 state may have been present in the crystals used for X-ray analysis because of extensive dark adaptation prior to data collection.

The first step in our analysis was to determine whether the proposed OEC model reproduces the experimental EXAFS of the S_1 state,[27] as simulated by using the *ab initio* real space Green's function approach implemented in FEFF (version 8.30),[28] because EXAFS measurements use small X-ray doses per irradiated area, leading to negligible photoreduction of the OEC.[27,29] For the EXAFS simulations (detailed in the

Received: January 29, 2015
Revised: February 18, 2015
Published: February 24, 2015

ACS Publications © 2015 American Chemical Society

DOI: 10.1021/acs.biochem.5b00089
Biochemistry 2015, 54, 1713−1716

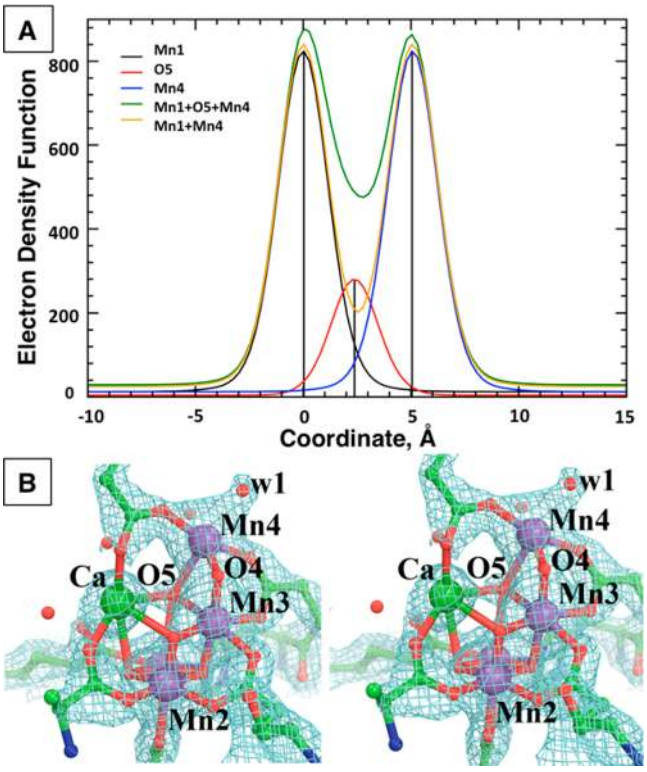

Figure 1. (A) Simulated electron density profile of the Mn1−O5−Mn4 coordinate and (B) stereo diagram of weighted $F_{obs} - F_{calc}$ maps using the observed structure factors and corresponding model phases contoured at 2.5 σ for 4UB8, monomer B.

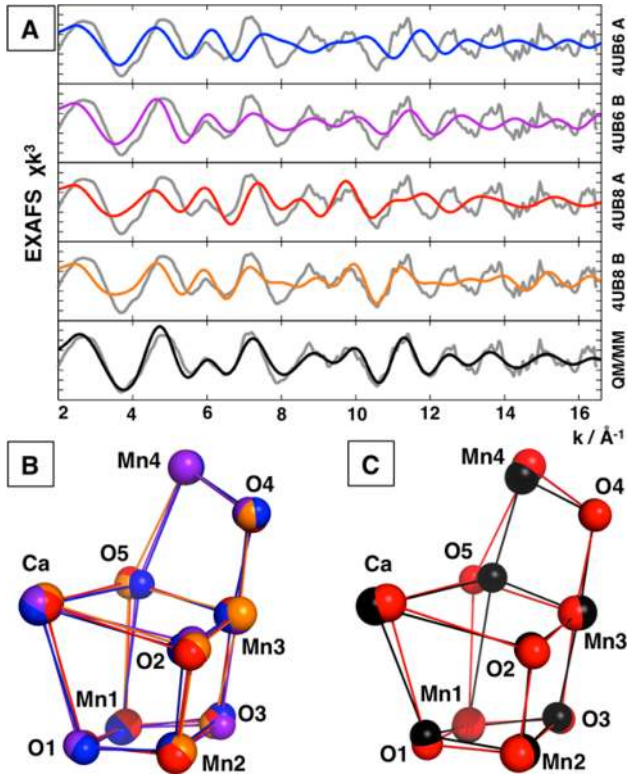

Figure 2. (A) EXAFS spectra simulated from 4UB6 monomer A (blue), 4UB6 monomer B (purple), 4UB8 monomer A (red), and 4UB8 monomer B (orange)[6] compared to the experimental[27] S_1 spectrum (gray). The simulated EXAFS spectrum of our S_1 QM/MM model[19] is shown in black for comparison. (B) Overlay of OEC atoms from 4UB6 monomer A (blue), 4UB6 monomer B (purple), 4UB8 monomer A (red), and 4UB8 monomer B (orange). (C) Overlay of OEC atoms from 4UB8 monomer A (red) and our S_1 QM/MM model (black).

Supporting Information), we used the coordinates from the two data sets (4UB6 and 4UB8) for both monomers A and B of PSII. We then compared the simulated EXAFS spectra to experimental EXAFS measurements of the S_1 state recorded at 20 K.[27,29] We note that room-temperature and cryogenic EXAFS measurements of the S_1 state are strikingly similar.[18,30]

Figure 2A shows that the spectra obtained with the OEC model of monomers A and B do not match the experimental S_1 EXAFS spectrum, in agreement with the recent work.[18] (Figure S1 of the Supporting Information shows the corresponding results in reduced distance space.) In addition, we note that the two monomers are slightly different and predict different EXAFS spectra.

Alignment of the OEC in the two data sets of the two monomers allows for a close inspection of the structural differences among the four reported OEC structures (Figure 2B and Table 1). Table 1 compares the root-mean-square deviations (rmsd's) upon pairwise alignment of all 10 atoms of the $CaMn_4O_5$ OEC core. We note that, on average, the rmsd from alignment of O atoms is 26% *higher* than the average rmsd of all 10 atoms, while the alignment of Mn is 39% *lower* (inclusion of the Ca atom makes it 36% *lower*). Clearly, there is more uncertainty in the positions of O atoms than in the positions of heavier Mn and Ca centers. We hypothesize that the lower precision in the position of O atoms is due to the limited spatial resolution of those atoms in the OEC structures at the given nominal experimental resolution.

To analyze the intrinsic uncertainty in the position of O atoms, we consider the OEC structure from monomer B of 4UB8, which has a Mn4−O5 distance of 2.38 Å and a Mn1−O5 distance of 2.70 Å. The reported *B* factors are 24.16 Å^2 for Mn4, 16.73 Å^2 for O5, and 21.36 Å^2 for Mn1. Using these distances and *B* factors at a resolution of 1.95 Å, we simulated the error-free electron density profile for the Mn4−O5−Mn1

Table 1. rmsd's (in angstroms) upon Pairwise Alignment of the OEC Core Atoms in the 4UB6 (monomers A and B) and 4UB8 (monomers A and B) Structures, According to All 10 Atoms in the $CaMn_4O_5$ Core (OEC), Only Mn and Ca Atoms (Ca and Mn1−Mn4), Only Mn Atoms (Mn1−Mn4), and Only O Atoms (O1−O5)

		4UB6 A	4UB6 B	4UB8 A	4UB8 B
OEC	4UB6 A	0			
	4UB6 B	0.125	0		
	4UB8 A	0.092	0.120	0	
	4UB8 B	0.127	0.089	0.110	0
Ca, Mn1-Mn4	4UB6 A	0			
	4UB6 B	0.055	0		
	4UB8 A	0.070	0.074	0	
	4UB8 B	0.085	0.055	0.084	0
Mn1-Mn4	4UB6 A	0			
	4UB6 B	0.049	0		
	4UB8 A	0.064	0.070	0	
	4UB8 B	0.079	0.049	0.091	0
O1-O5	4UB6 A	0			
	4UB6 B	0.119	0		
	4UB8 A	0.183	0.162	0	
	4UB8 B	0.175	0.117	0.080	0

DOI: 10.1021/acs.biochem.5b00089
Biochemistry 2015, 54, 1713−1716

coordinate, as shown in Figure 1, for a linear coordinate connecting the three atoms. It is clear that the Mn peaks dominate the signal because Mn has three times more electrons than O, leading to significant overlap and poor spatial resolution of the positions of the O atom (Figure S4 of the Supporting Information shows the simulated electron density profiles for atoms with similar electron counts and smaller *B* factors). The OEC μ-oxo bridges corresponding to (O4), (O1, O2, O3), and (O5) are surrounded by two, three, and four metal centers, respectively, with high electron-density signals. Therefore, they are more poorly resolved than the terminal waters bound to Mn4 and Ca, connected to only one metal and with a longer coordination bond (Figure 1B).

The spatial resolution of light atoms next to heavy atoms is known to be extremely difficult, as documented in other metalloproteins, such as the interstitial carbon atom inside the nitrogenase FeMo cofactor, which required a resolution of 1.16 Å to resolve it.[31,32] In fact, this light atom was not discovered in structures at 1.55 Å resolution because it was completely masked by negative Fourier truncation ripple effects. In our study, we find that the light O atoms next to Mn atoms, on the opposite, may suffer from positive Fourier truncation ripple effects (see Figure S4F of the Supporting Information) that can deceptively lead to a better resolution of the O atoms but distort their positions.

In addition to error arising from the O atom positions, we find that the Mn−Mn distances are inconsistent with EXAFS measurements of the S_1 state. The S_1 state has three Mn−Mn distances of 2.7−2.8 Å and one that is ∼3.2 Å.[29,30,33,34] As shown in Table 2, the Mn1−Mn2, Mn2−Mn3, and Mn1−Mn3 distances are similar to both experimental EXAFS and our previously reported QM/MM model of S_1 (Figure 2C), with the largest average deviation being 0.055 Å. However, the Mn3−Mn4 vector is significantly (0.170 Å) longer, which cannot be ascribed to poor resolution. Interestingly, the Mn3−Mn4 distance is one that is expected to become longer when S_1 is reduced to S_0 because of the change in oxidation state of Mn3 from Mn^{4+} to Mn^{3+} and the orientation of the resulting Jahn−Teller axis toward O5.[19]

Table 2. Mn−Mn Distances (in angstroms) in Monomers A and B in the 4UB6 and 4UB8 Data Sets[6] and Average Deviations from Our Previously Reported S_1 and S_0 QM/MM Models[19]

	Mn1-Mn2	Mn2-Mn3	Mn1-Mn3	Mn3-Mn4
4UB6 A	2.61	2.67	3.18	2.83
4UB6 B	2.67	2.7	3.24	2.86
4UB8 A	2.68	2.77	3.12	2.83
4UB8 B	2.74	2.71	3.33	2.88
$S_{1QM/MM}$	2.73	2.76	3.26	2.68
$\Delta(S_{1QM/MM}\text{-X})$	0.055	0.047	0.043	-0.17
$S_{0QM/MM}$	2.73	2.77	3.20	2.95
$\Delta(S_{0QM/MM}\text{-X})$	0.055	0.057	-0.017	0.100

The average Mn3−Mn4 distance of 2.85 Å in the radiation-damage-free OEC structures may be explained if a significant population of reaction centers was poised in S_0 instead of S_1. Such sample reduction may occur spontaneously during sample preparation and would not be the result of X-ray-induced reduction. PSII that has been dark adapted for several minutes typically contains ∼25% S_0 and ∼75% S_1 with Y_D oxidized ($Y_D^{\bullet}$).[4] On the time scale of hours, S_0 is oxidized by $Y_D^{\bullet}$ to produce a population that approaches 100% S_1 with Y_D reduced.[35] While kinetically unfavored, S_1 may be reduced to S_0 over very long time periods of dark adaptation. For example, the PSII samples used in ref 6 were crystallized over approximately 1 week in the dark.

As detailed in the Supporting Information, we have also simulated the metal-only EXAFS spectra of the four OEC structures and compared them to metal-only EXAFS spectra of QM/MM models of S_0 and S_1[19] in an effort to minimize the influence of O atoms on the model. However, only marginal improvements in fits were observed for the four OEC structures as compared to linear combinations of S_0 and S_1 spectra (see the Supporting Information).

We conclude that the four OEC structures in ref 6 reflect slightly different combinations of S_0 and S_1 with a high degree of uncertainty in the position of O atoms. A substantial population of S_0 may have accumulated during the very long dark incubations of the samples and is reflected in elongated Mn3−Mn4 distances. The long Mn−O5 bond distances observed in the reported structures may be attributed to the protonated form of O5 as predicted for S_0.[19] Furthermore, we have shown that the positions of O atoms close to Mn centers are difficult to resolve even at 1.95 Å, so their assigned positions are likely dependent on the model used to fit the electron density map.

■ ASSOCIATED CONTENT

Supporting Information

Description and analysis of EXAFS simulations and analysis of electron density maps. This material is available free of charge via the Internet at http://pubs.acs.org.

■ AUTHOR INFORMATION

Corresponding Authors

*E-mail: victor.batista@yale.edu. Phone: (203) 432-6672. Fax: (203) 432-6144.

*E-mail: gary.brudvig@yale.edu. Phone: (203) 432-5202. Fax: (203) 432-6144.

Funding

This material is based upon work supported by the U.S. Department of Energy, Office of Science, Office of Basic Energy Sciences, Division of Chemical Sciences, Geosciences, and Biosciences, via Grants DESC0001423 (V.S.B.) for computational work and DE-FG0205ER15646 (G.W.B.) for experimental work. Crystallographic work was supported by National Institutes of Health Project Grant P01 GM022778 and funding from the Steitz Center for Structural Biology, Gwangju Institute of Science and Technology, Republic of Korea.

Notes

The authors declare no competing financial interest.

■ ACKNOWLEDGMENTS

We acknowledge Dr. Christian F. A. Negre for making an invaluable contribution to the EXAFS simulation methodology.

■ REFERENCES

(1) McEvoy, J. P., and Brudvig, G. W. (2006) *Chem. Rev. 106*, 4455−4483.

(2) Cox, N., and Messinger, J. (2013) *Biochim. Biophys. Acta 1827*, 1020−1030.

DOI: 10.1021/acs.biochem.5b00089
Biochemistry 2015, 54, 1713−1716

(3) Joliot, P., and Kok, B. (1975) Oxygen evolution in photosynthesis. In *Bioenergetics of Photosynthesis* (Govindjee, Ed.) pp 387−412, Academic Press, New York.
(4) Kok, B., Forbush, B., and McGloin, M. (1970) *Photochem. Photobiol. 11*, 457−475.
(5) Umena, Y., Kawakami, K., Shen, J.-R., and Kamiya, N. (2011) *Nature 473*, 55−60.
(6) Suga, M., Akita, F., Hirata, K., Ueno, G., Murakami, H., Nakajima, Y., Shimizu, T., Yamashita, K., Yamamoto, M., Ago, H., and Shen, J.-R. (2015) *Nature 517*, 99−103.
(7) Forbush, B., Kok, B., and McGloin, M. P. (1971) *Photochem. Photobiol. 14*, 307−321.
(8) Grabolle, M., and Dau, H. (2005) *Biochim. Biophys. Acta 1708*, 209−218.
(9) Ferreira, K. N., Iverson, T. M., Maghlaoui, K., Barber, J., and Iwata, S. (2004) *Science 303*, 1831−1838.
(10) Guskov, A., Kern, J., Gabdulkhakov, A., Broser, M., Zouni, A., and Saenger, W. (2009) *Nat. Struct. Mol. Biol. 16*, 334−342.
(11) Kamiya, N., and Shen, J. R. (2003) *Proc. Natl. Acad. Sci. U.S.A. 100*, 98−103.
(12) Loll, B., Kern, J., Saenger, W., Zouni, A., and Biesiadka, J. (2005) *Nature 438*, 1040−1044.
(13) Zouni, A., Witt, H. T., Kern, J., Fromme, P., Krauß, N., Saenger, W., and Orth, P. (2001) *Nature 409*, 739−743.
(14) Yano, J., Kern, J., Irrgang, K. D., Latimer, M. J., Bergmann, U., Glatzel, P., Pushkar, Y., Biesiadka, J., Loll, B., Sauer, K., Messinger, J., Zouni, A., and Yachandra, V. K. (2005) *Proc. Natl. Acad. Sci. U.S.A. 102*, 12047−12052.
(15) Galstyan, A., Robertazzi, A., and Knapp, E. W. (2012) *J. Am. Chem. Soc. 134*, 7442−7449.
(16) Luber, S., Rivalta, I., Umena, Y., Kawakami, K., Shen, J.-R., Kamiya, N., Brudvig, G. W., and Batista, V. S. (2011) *Biochemistry 50*, 6308−6311.
(17) Pantazis, D. A., Ames, W., Cox, N., Lubitz, W., and Neese, F. (2012) *Angew. Chem., Int. Ed. 51*, 9935−9940.
(18) Davis, K. M., and Pushkar, Y. (2015) *J. Phys. Chem. B 119*, 3492−3498.
(19) Pal, R., Negre, C. F. A., Vogt, L., Pokhrel, R., Ertem, M. Z., Brudvig, G. W., and Batista, V. S. (2013) *Biochemistry 52*, 7703−7706.
(20) Neutze, R., Wouts, R., van der Spoel, D., Weckert, E., and Hajdu, J. (2000) *Nature 406*, 752−757.
(21) Chapman, H. N., Fromme, P., Barty, A., White, T. A., Kirian, R. A., Aquila, A., Hunter, M. S., Schulz, J., DePonte, D. P., Weierstall, U., et al. (2011) *Nature 470*, 73−77.
(22) Kern, J., Alonso-Mori, R., Hellmich, J., Tran, R., Hattne, J., Laksmono, H., et al. (2012) *Proc. Natl. Acad. Sci. U.S.A. 109*, 9721−9726.
(23) Kern, J., Alonso-Mori, R., Tran, R., Hattne, J., Gildea, R. J., Echols, N., et al. (2013) *Science 340*, 491−495.
(24) Kupitz, C., Basu, S., Grotjohann, I., Fromme, R., Zatsepin, N. A., Rendek, K. N., Hunter, M. S., et al. (2014) *Nature 513*, 261−265.
(25) Kern, J., Tran, R., Alonso-Mori, R., Koroidov, S., Echols, N., Hattne, J., Ibrahim, M., Gul, S., Laksmono, H., Sierra, R. G., Gildea, R. J., Han, G., Hellmich, J., Lassalle-Kaiser, B., Chatterjee, R., Brewster, A. S., Stan, C. A., Glöckner, C., Lampe, A., DiFiore, D., Milathianaki, D., Fry, A. R., Seibert, M. M., Koglin, J. E., Gallo, E., Uhlig, J., Sokaras, D., Weng, T.-C., Zwart, P. H., Skinner, D. E., Bogan, M. J., Messerschmidt, M., Glatzel, P., Williams, G. J., Boutet, S., Adams, P. D., Zouni, A., Messinger, J., Sauter, N. K., Bergmann, U., Yano, J., and Yachandra, V. K. (2014) *Nat. Commun. 5*, 4371.
(26) Askerka, M., Wang, J., Brudvig, G. W., and Batista, V. S. (2014) *Biochemistry 53*, 6860−6862.
(27) Grundmeier, A., and Dau, H. (2012) *Biochim. Biophys. Acta 1817*, 88−105.
(28) Ankudinov, A. L., Bouldin, C. E., Rehr, J. J., Sims, J., and Hung, H. (2002) *Phys. Rev. B 65*, 104107.
(29) Dau, H., Grundmeier, A., Loja, P., and Haumann, M. (2008) *Philos. Trans. R. Soc., B 363*, 1237−1243.
(30) Haumann, M., Muller, C., Liebisch, P., Iuzzolino, L., Dittmer, J., Grabolle, M., Neisius, T., Meyer-Klaucke, W., and Dau, H. (2005) *Biochemistry 44*, 1894−1908.
(31) Einsle, O., Tezcan, F. A., Andrade, S. L. A., Schmid, B., Yoshida, M., Howard, J. B., and Rees, D. C. (2002) *Science 297*, 1696−1700.
(32) Spatzal, T., Aksoyoglu, M., Zhang, L. M., Andrade, S. L. A., Schleicher, E., Weber, S., Rees, D. C., and Einsle, O. (2011) *Science 334*, 940.
(33) Yano, J., Kern, J., Sauer, K., Latimer, M. J., Pushkar, Y., Biesiadka, J., Loll, B., Saenger, W., Messinger, J., Zouni, A., and Yachandra, V. K. (2006) *Science 314*, 821−825.
(34) Dau, H., and Haumann, M. (2008) *Coord. Chem. Rev. 252*, 273−295.
(35) Styring, S., and Rutherford, A. W. (1987) *Biochemistry 26*, 2401−2405.

DOI: 10.1021/acs.biochem.5b00089
Biochemistry 2015, 54, 1713−1716